

# Models of cuspy triaxial stellar systems – II. Regular orbits

J. C. Muzzio,<sup>1</sup>★ H. D. Navone<sup>2</sup> and A. F. Zorzi<sup>2</sup>

<sup>1</sup>*Instituto de Astrofísica de La Plata (CONICET La Plata–UNLP) and Facultad de Ciencias Astronómicas y Geofísicas, Universidad Nacional de La Plata, La Plata 1900, Argentina*

<sup>2</sup>*Instituto de Física de Rosario (CONICET–UNR) and Facultad de Ciencias Exactas, Ingeniería y Agrimensura, Universidad Nacional de Rosario, Rosario 2000, Argentina*

Accepted 2012 October 18. Received 2012 October 14; in original form 2012 August 21

## ABSTRACT

In the first paper of this series we used the  $N$ -body method to build a dozen cuspy ( $\gamma \simeq 1$ ) triaxial models of stellar systems, and we showed that they were highly stable over time intervals of the order of a Hubble time, even though they had very large fractions of chaotic orbits (more than 85 per cent in some cases). The models were grouped in four sets, each one comprising models morphologically resembling E2, E3, E4 and E5 galaxies, respectively. The three models within each set, although different, had the same global properties and were statistically equivalent. In the present paper we use frequency analysis to classify the regular orbits of those models. The bulk of those orbits are short-axis tubes, with a significant fraction of long-axis tubes (LATs) in the E2 models that decreases in the E3 and E4 models to become negligibly small in the E5 models. Most of the LATs in the E2 and E3 models are outer LATs, but the situation reverses in the E4 and E5 models where the few LATs are mainly inner LATs. As could be expected for cuspy models, most of the boxes are resonant orbits, i.e. boxlets. Nevertheless, only the  $(x, y)$  fishes of models E3 and E4 amount to about 10 per cent of the regular orbits, with most of the fractions of the other boxlets being of the order of 1 per cent or less.

**Key words:** methods: numerical – galaxies: elliptical and lenticular, cD – galaxies: kinematics and dynamics.

## 1 INTRODUCTION

The observational evidence, both statistical (Ryden 1996) and on individual galaxies (Statler et al. 2004), indicates that at least some elliptical galaxies are triaxial and not merely rotationally symmetric. Besides, their surface brightness increases towards the centre, forming a cusp (Crane et al. 1993; Moller, Stiavelli & Zeilinger 1995) that reveals a mass concentration, and perhaps the presence of a black hole, there. Thus, the need of triaxial and cuspy models to represent elliptical galaxies seems to be warranted.

Triaxial models of stellar systems with smooth cores harbour four major families of regular orbits: boxes, short-axis tubes (SATs) and inner and outer long-axis tubes (ILATs and OLATs, respectively); see e.g. de Zeeuw (1985) or Statler (1987). Significant resonant orbit families, called boxlets, were found in the singular logarithmic potential (Binney 1982; Miralda-Escudé & Schwarzschild 1989) and, in general, they tend to replace the box orbits in models with central cusps. Although chaotic orbits were originally thought to make only a minor contribution to the orbital content of triaxial models, they were later recognized to arise naturally in those models, especially in cuspy ones (Kandrup & Siopis 2003).

In a recent paper (Zorzi & Muzzio 2012, hereafter Paper I) we have presented self-consistent models of cuspy triaxial stellar systems obtained using the  $N$ -body method. The models are morphologically similar to elliptical galaxies of Hubble types E2–E5, with de Vaucouleurs density profiles. We showed that they were very stable over time intervals of the order of one Hubble time, even though they contained extremely high fractions of chaotic orbits (higher than 85 per cent in half of the models). Thus, the usual idea that the regular orbits provide the backbone of stellar systems is in doubt for these models. In the present paper we use frequency analysis techniques to classify the regular orbits found in our previous investigation, in order to determine which kinds of regular orbits are present in the models of Paper I and in which proportions they appear.

In the next section we describe the models and the classification technique. Section 3 presents our results, and Section 4 summarizes our conclusions.

## 2 MODELS AND TECHNIQUES

### 2.1 The models

A detailed explanation of how the models were built is given in Paper I. Briefly, the recipe of Aguilar & Merritt (1990) was used, randomly creating a spherical distribution of  $10^6$  particles with a

★E-mail: jcmuzzio@fcaglp.unlp.edu.ar

**Table 1.** Orbital classification results.

Model	Total	Chaotic (per cent)	BBL (per cent)	SAT (per cent)	ILAT (per cent)	OLAT (per cent)
E2a	1113	0.54 ± 0.22	9.88 ± 0.89	54.72 ± 1.49	3.14 ± 0.52	31.72 ± 1.39
E2b	1057	0.28 ± 0.16	7.66 ± 0.82	51.66 ± 1.54	3.69 ± 0.58	36.71 ± 1.48
E2c	1101	0.54 ± 0.22	6.63 ± 0.75	59.58 ± 1.48	2.27 ± 0.45	30.97 ± 1.39
E3a	696	6.03 ± 0.90	20.26 ± 1.52	57.76 ± 1.87	7.04 ± 0.97	8.91 ± 1.08
E3b	687	3.20 ± 0.67	23.00 ± 1.61	53.86 ± 1.90	6.84 ± 0.96	13.10 ± 1.29
E3c	520	4.04 ± 0.86	25.58 ± 1.91	53.85 ± 2.18	6.54 ± 1.08	10.00 ± 1.32
E4a	594	2.02 ± 0.58	32.15 ± 1.92	59.76 ± 2.01	5.05 ± 0.90	1.01 ± 0.41
E4b	576	2.78 ± 0.68	31.42 ± 1.93	60.24 ± 2.04	4.69 ± 0.88	0.87 ± 0.39
E4c	575	2.09 ± 0.60	26.78 ± 1.85	66.43 ± 1.97	4.00 ± 0.82	0.70 ± 0.35
E5a	984	0.41 ± 0.20	8.03 ± 0.87	91.06 ± 0.91	0.51 ± 0.23	0.00 ± 0.00
E5b	1047	1.15 ± 0.33	6.21 ± 0.75	92.17 ± 0.83	0.48 ± 0.21	0.00 ± 0.00
E5c	949	0.84 ± 0.30	4.32 ± 0.66	94.10 ± 0.76	0.63 ± 0.26	0.11 ± 0.11

**Table 2.** Orbital classification results per energy bin.

Model	Energy bin (per cent)	<i>a</i>	<i>b/a</i>	<i>c/a</i>	Total	Chaotic (per cent)	BBL (per cent)	SAT (per cent)	ILAT (per cent)	OLAT (per cent)
E2	0–20	0.068	0.754	0.601	578	0.00 ± 0.00	14.53 ± 1.47	74.39 ± 1.82	10.90 ± 1.30	0.17 ± 0.17
	20–40	0.151	0.795	0.704	325	0.00 ± 0.00	15.38 ± 2.00	78.15 ± 2.29	3.38 ± 1.00	3.08 ± 0.96
	40–60	0.251	0.853	0.799	455	0.00 ± 0.00	7.91 ± 1.27	55.16 ± 2.33	0.88 ± 0.44	36.04 ± 2.25
	60–80	0.512	0.891	0.847	704	0.00 ± 0.00	4.69 ± 0.80	51.56 ± 1.88	0.57 ± 0.28	43.18 ± 1.87
	80–100	1.145	0.945	0.930	1209	1.24 ± 0.32	5.05 ± 0.63	42.43 ± 1.42	1.41 ± 0.34	49.88 ± 1.44
E3	0–20	0.064	0.725	0.570	454	0.00 ± 0.00	11.89 ± 1.52	78.19 ± 1.94	9.91 ± 1.40	0.00 ± 0.00
	20–40	0.151	0.711	0.557	223	0.00 ± 0.00	27.80 ± 3.00	69.51 ± 3.08	1.79 ± 0.89	0.90 ± 0.63
	40–60	0.234	0.800	0.671	191	0.00 ± 0.00	22.51 ± 3.02	69.11 ± 3.34	2.09 ± 1.04	6.28 ± 1.76
	60–80	0.515	0.819	0.707	301	0.00 ± 0.00	19.60 ± 2.29	61.46 ± 2.81	2.33 ± 0.87	16.61 ± 2.15
	80–100	2.449	0.850	0.813	734	11.58 ± 1.18	29.16 ± 1.68	30.65 ± 1.70	9.54 ± 1.08	19.07 ± 1.45
E4	0–20	0.056	0.736	0.582	421	0.00 ± 0.00	18.53 ± 1.89	69.36 ± 2.25	12.11 ± 1.59	0.00 ± 0.00
	20–40	0.135	0.694	0.504	256	0.00 ± 0.00	28.12 ± 2.81	69.92 ± 2.87	1.56 ± 0.78	0.39 ± 0.39
	40–60	0.218	0.750	0.557	297	0.00 ± 0.00	27.95 ± 2.60	69.70 ± 2.67	2.36 ± 0.88	0.00 ± 0.00
	60–80	0.383	0.780	0.595	409	0.00 ± 0.00	21.27 ± 2.02	76.53 ± 2.10	0.98 ± 0.49	1.22 ± 0.54
	80–100	2.557	0.789	0.701	362	11.05 ± 1.65	56.91 ± 2.60	25.69 ± 2.30	3.87 ± 1.01	2.49 ± 0.82
E5	0–20	0.051	0.839	0.579	676	0.00 ± 0.00	5.03 ± 0.84	92.75 ± 1.00	2.07 ± 0.55	0.15 ± 0.15
	20–40	0.124	0.811	0.497	602	0.00 ± 0.00	2.49 ± 0.64	97.18 ± 0.68	0.33 ± 0.23	0.00 ± 0.00
	40–60	0.216	0.807	0.501	483	0.00 ± 0.00	5.59 ± 1.05	94.41 ± 1.05	0.00 ± 0.00	0.00 ± 0.00
	60–80	0.358	0.808	0.512	537	0.00 ± 0.00	6.52 ± 1.07	93.48 ± 1.07	0.00 ± 0.00	0.00 ± 0.00
	80–100	0.993	0.899	0.573	682	3.52 ± 0.71	10.85 ± 1.19	85.63 ± 1.34	0.00 ± 0.00	0.00 ± 0.00

density distribution inversely proportional to the distance to the centre and a Gaussian velocity distribution, and following its collapse with the code of Hernquist & Ostriker (1992); the resulting triaxial system is a consequence of the radial orbit instability. The gravitational constant,  $G$ , the radius of the sphere and the total mass are all set equal to 1. The models were rotated to have the major, intermediate and minor axes of their moment of inertia tensor aligned with the  $x$ ,  $y$  and  $z$  coordinate axes, respectively (hereafter the corresponding velocity components are dubbed  $u$ ,  $v$  and  $w$ , respectively). Particles with energies close to, or larger than, zero were eliminated and the models were allowed to relax to make sure they had reached equilibrium. Tables 1 and 2 of Paper I give the main properties of the models and, in particular, crossing times ( $T_{\text{cr}}$ ) are of the order of 0.5 time units (t.u.); the Hubble time was found to be of the order of 100 t.u., or about  $200T_{\text{cr}}$ . The major, intermediate and minor axes of the models ( $a$ ,  $b$  and  $c$ , respectively) were obtained from the mean square values of the  $x$ ,  $y$  and  $z$  coordinates, respectively, taking the 20, 40, ..., 100 per cent most tightly bound particles. The major semi-axes and the semi-axes ratios change with the orbital energy

limit and are given in table 2 of Paper I. The Hubble type was estimated from the  $c/a$  ratio of the 80 most tightly bound particles, but it should be noticed that triaxiality ( $T = (a^2 - b^2)/(a^2 - c^2)$ ), given in table 1 of Paper I, goes from about 0.73 (i.e. not too far from being prolate) for the E2 models to about 0.47 (i.e. close to maximum triaxiality) for the E5 ones. To aid the reader, we give the  $a$ ,  $b/a$  and  $c/a$  values also in Table 2 of the present paper but, in this case, the results for the three models of each group were bunched together and they were computed in energy bins, instead of groups of the 20, 40, ..., 100 per cent most bounded particles as in Paper I. The density distributions follow the de Vaucouleurs law and all the models are cuspy, with central densities proportional to  $r^{-\gamma}$  and  $\gamma \simeq 1$ . The 12 models are divided in four groups, E2, E3, E4 and E5, named after the elliptical galaxy classes that correspond to their axial ratios. Three models ( $a$ ,  $b$  and  $c$ ) were created for each group using different seed numbers for the random number generator, so that they are statistically equivalent; in fact, as shown in Paper I, the macroscopic properties of the three models in each group turned out to be essentially the same.

We showed in Paper I that all the models are highly stable over time intervals of the order of a Hubble time. Their orbital structure is dominated by chaotic orbits, with regular orbits amounting to little more than 20 per cent in models E2 and E5 and to less than 15 per cent in models E3 and E4.

## 2.2 Frequency analysis and regular orbit classification

As in our previous papers (Muzzio 2006; Aquilano et al. 2007; Muzzio, Navone & Zorzi 2009), the modified Fourier transform code of Sidlichovský & Nesvorný (1997) (a copy can be obtained at [www.boulder.swri.edu/~davidn](http://www.boulder.swri.edu/~davidn)) was used for the frequency analysis. In Paper I the positions and velocities of about 5000 bodies were randomly selected from each model and adopted as initial conditions for the computation of the Lyapunov exponents, which allowed us to separate the regular from the chaotic orbits. For the 9899 orbits deemed there as regular, we adopted here those same initial positions and velocities to compute the corresponding orbits and we obtained the fundamental frequencies for each coordinate,  $F_x$ ,  $F_y$  and  $F_z$ , performing the frequency analysis on the complex variables  $x + iy$ ,  $y + iv$  and  $z + iw$ , respectively; these were derived from 8192 points equally spaced in time obtained integrating the regular orbits over 300 radial periods. In this way, as indicated by Muzzio (2006), frequencies can be obtained with a precision better than  $10^{-9}$  for isolated lines; nevertheless, the precision is much lower when there are nearby lines and the practical limit of  $2 \times 10^{-4}$  for the precision, adopted in our previous works, is also used here.

The orbits were then classified as boxes and boxlets (BBLs), SATs, ILATs and OLATs using the method of Kalapotharakos & Voglis (2005), with the improvements introduced by Muzzio (2006), Aquilano et al. (2007) and Muzzio et al. (2009). The original method took the frequency of the largest amplitude component in each coordinate as the fundamental frequency for that coordinate but, as shown by Binney & Spergel (1982) and Muzzio (2006), respectively, the libration of some orbits and the extreme elongation of others make necessary to adopt other frequencies as the fundamental ones, so that some of the improvements deal with those cases. Furthermore, Aquilano et al. (2007) showed that one has to take into account the energy of the orbit, in addition to the  $F_x/F_z$  ratio used by Kalapotharakos & Voglis (2005), to separate ILATs from OLATs and that is another improvement of the original method. Finally, we searched for resonances among the fundamental frequencies of the BBLs in order to separate the boxes from the boxlets.

## 3 RESULTS AND ANALYSIS

Of the 9899 orbits regarded as regular in Paper I, 180 yielded anomalous values of their fundamental frequencies, i.e. frequencies that did not obey that  $F_x \leq F_y \leq F_z$  or whose  $F_y/F_z$  or  $F_x/F_z$  ratios placed them at odd locations on the frequency map. Visual inspection of their spectra showed that most of them were typical of chaotic orbits, with lines of similar frequencies and amplitudes. We checked that possibility obtaining the finite time Lyapunov characteristic numbers (FT-LCNs, see Paper I for details) of those orbits using an integration time of 100 000 t.u., i.e. 10 times longer than that used in Paper I. The limiting value to separate regular from chaotic orbits with the longer integration time was found to be  $0.00020$  (t.u.)<sup>-1</sup>, while in Paper I it was  $0.00180$  (t.u.)<sup>-1</sup>. Of the 180 suspicious orbits, 164 turned out to be actually chaotic and were eliminated from the subsequent analysis. Plots of the remaining 16 orbits showed them to be normal tubes, but most had highly elongated orbits so that, as

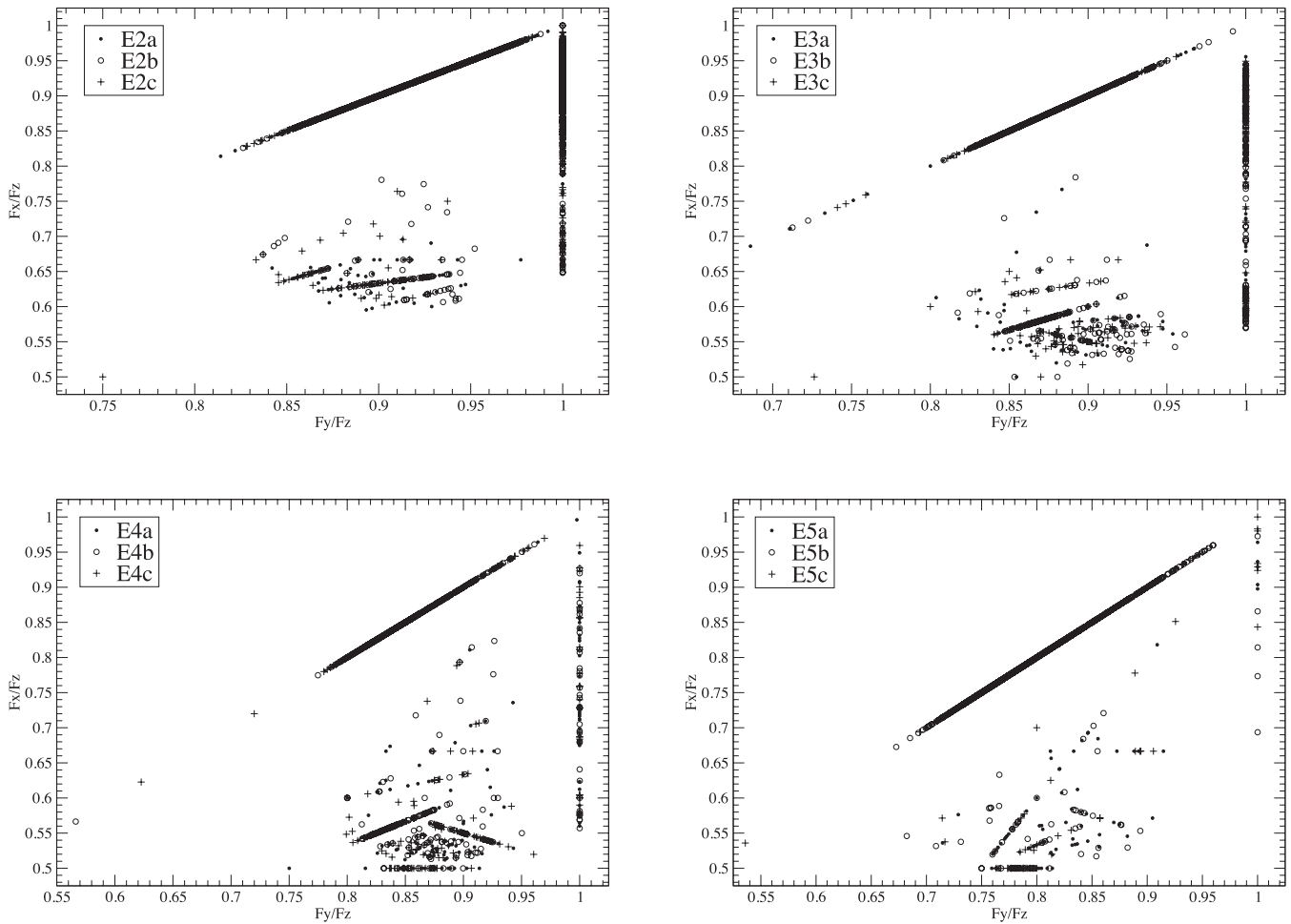
indicated by Muzzio (2006), their fundamental frequencies should not be taken as those corresponding to the largest amplitude. In fact, relaxing the condition that allows us to adopt a frequency different from that of largest amplitude as the fundamental frequency, let our classification code to automatically select the right frequencies, but this procedure is risky and may spoil the classification of other orbits, so that we preferred to select the fundamental frequencies for those few orbits from visual inspection of their frequency spectra.

Fig. 1 presents the frequency maps for each group and, within each panel, different symbols are used for each one of the three statistically equivalent models. The plots are bound by the  $F_x/F_z = F_y/F_z$  correlation, corresponding to the SATs, and the  $F_y/F_z = 1$  correlation, corresponding to the LATs. Besides, several other correlations, corresponding to different boxlets, are evident on the plots. Within each panel there is generally good agreement among the results from the different models within each group. To aid the reader, the main resonances that stand out in Fig. 1 are identified in Fig. 2.

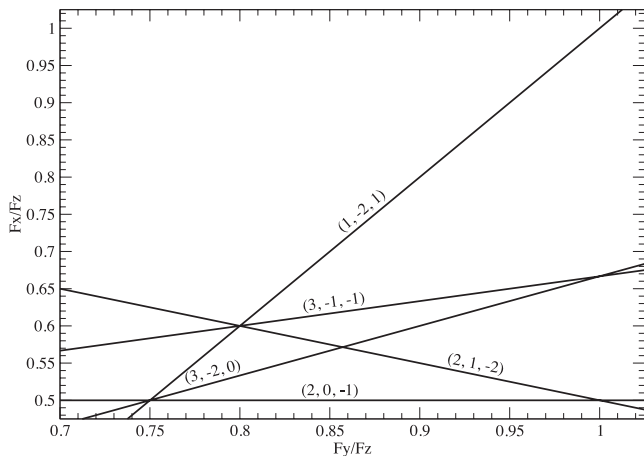
Except for the 16 orbits mentioned before, whose fundamental frequencies were obtained from visual inspection of their spectra, all the others were automatically classified by our code. LATs were segregated into ILATs and OLATs using  $F_x/F_z$  versus orbital energy plots, as explained by Aquilano et al. (2007). Table 1 summarizes the classification results. It gives, for each model, the total number of regular orbits found in Paper I, and the percentages of them that turned out to be chaotic with the longer integration interval, and that were classified as BBLs, SATs, ILATs and OLATs; the statistical errors have been estimated from the binomial distribution, as in our previous papers.

Table 2 presents the results of the classification for the orbits grouped in orbital energy bins and, since the numbers are small, the results of the three models of each group have been bunched together. The first column gives the group and the second one gives the energy range of the bin; columns three through five give the major semi-axis and the semi-axes ratios corresponding to the bin; the other columns are as in Table 1 except that the rows correspond to the energy bins rather than to the different models.

Although we had found before (Muzzio et al. 2009) that some orbits deemed to be regular from their FT-LCNs turned out to be chaotic during the orbital classification, the percentages shown in Tables 1 and 2 are worrisome. As a check, for all the 576 orbits of model E4b classified as regular in Paper I, we obtained the FT-LCNs using the 10 times longer interval. For 172 orbits the new FT-LCNs turned out to be larger than the new limiting value of  $0.00020$  (t.u.)<sup>-1</sup>, i.e. they should be regarded as chaotic. Nevertheless, only 33 of those had FT-LCNs larger than the limiting value of  $0.00180$  (t.u.)<sup>-1</sup> of Paper I. In other words, only  $5.73 \pm 0.31$  per cent of the ‘regular’ orbits of Paper I turned out to be sticky orbits that actually had FT-LCNs larger than the limit adopted there. In addition, another  $24.13 \pm 0.18$  per cent were weakly chaotic orbits whose FT-LCNs were simply below the detection limit used in Paper I. Considering this result, the percentages of chaotic orbits of Table 1 are not very high, in all likelihood because they were found rather accidentally from oddities of the frequency analysis, but one should remember that they are just the tip of the iceberg and that any sample of regular orbits obtained using chaos indicators, such as the FT-LCNs, is bound to include a substantial amount of chaotic orbits as well. Fortunately, at least in our case, most of these are weakly chaotic orbits whose behaviour is not too different from that of regular orbits (Kalapotharakos & Voglis 2005), with sticky orbits that might exhibit a wilder behaviour being a minority only. The bulk



**Figure 1.** Frequency maps for models E2 (top left), E3 (top right), E4 (bottom left) and E5 (bottom right). Please note that the horizontal scale is different for each model.



**Figure 2.** Main resonances in the frequency maps.

of the sticky orbits (26 of them) were concentrated in the highest 20 per cent energy bin, while the numbers of weakly chaotic orbits raised steadily from the lowest (seven orbits) through the highest (56 orbits) energy bins.

Since the BBLs include both true boxes and resonant boxes (boxlets), it is important to segregate ones from the others. Thus, we searched for resonances obeying the relationship

$$lF_x + mF_y + nF_z = 0, \tag{1}$$

with  $l, m$  and  $n$  integers not all equal to zero. Since our computed frequencies are not exact, the above relationship can be fulfilled only approximately, and it is rather risky to search for resonances that involve very large integers, because the chance of finding spurious resonances is large. Therefore, we performed two searches, one limiting the integers to values smaller than or equal to 5, and another one rising that limit to 10. Since the numbers of the different kinds of resonant orbits are small, we bunched together the three different models of each group and the results are presented in Table 3 as percentages of the total number of regular orbits. These results can be compared with those in the equivalent tables from Aquilano et al. (2007) and Muzzio et al. (2009). The first line gives the percentage of BBLs and the second one the percentage of those that have no resonances in the search performed with integers up to 5, i.e. those that can be regarded as boxes at that level of the search. The following lines give the percentages of orbits which obey one single resonance and that have a percentage larger than 1 per cent in, at least, one model; those with smaller percentages were bunched together in the line labelled ‘Other’. The line before the last one gives the percentages of orbits that obey two resonances

**Table 3.** Percentages of boxes and boxlets.

Type	E2 (per cent)	E3 (per cent)	E4 (per cent)	E5 (per cent)
BBL	$8.07 \pm 0.48$	$22.70 \pm 0.96$	$30.14 \pm 1.10$	$6.21 \pm 0.44$
Boxes ( $\leq 5$ )	$0.79 \pm 0.16$	$3.89 \pm 0.44$	$2.98 \pm 0.41$	$0.23 \pm 0.09$
(1, -2, 1)	$0.15 \pm 0.07$	$0.16 \pm 0.09$	$0.46 \pm 0.16$	$1.07 \pm 0.19$
(2, 0, -1)	$0.00 \pm 0.00$	$0.26 \pm 0.12$	$3.09 \pm 0.41$	$1.71 \pm 0.24$
(2, 1, -2)	$0.00 \pm 0.00$	$2.31 \pm 0.34$	$3.78 \pm 0.46$	$0.40 \pm 0.12$
(3, -2, 0)	$0.76 \pm 0.15$	$8.57 \pm 0.64$	$10.43 \pm 0.73$	$0.64 \pm 0.15$
(3, -1, -1)	$3.15 \pm 0.31$	$1.26 \pm 0.26$	$1.09 \pm 0.25$	$0.27 \pm 0.09$
(3, -3, 1)	$0.03 \pm 0.03$	$0.47 \pm 0.16$	$0.86 \pm 0.22$	$0.00 \pm 0.00$
(4, -3, 0)	$1.47 \pm 0.21$	$0.32 \pm 0.13$	$0.23 \pm 0.11$	$0.13 \pm 0.07$
(5, -3, 0)	$0.00 \pm 0.00$	$0.16 \pm 0.09$	$0.97 \pm 0.24$	$0.00 \pm 0.00$
(5, -2, -1)	$0.00 \pm 0.00$	$1.05 \pm 0.23$	$0.69 \pm 0.20$	$0.13 \pm 0.07$
Other ( $\leq 5$ )	$1.22 \pm 0.19$	$1.84 \pm 0.31$	$2.69 \pm 0.39$	$0.81 \pm 0.16$
Two resonances ( $\leq 5$ )	$0.49 \pm 0.12$	$2.42 \pm 0.35$	$2.87 \pm 0.40$	$0.81 \pm 0.16$
Boxes ( $\leq 10$ )	$0.21 \pm 0.08$	$1.58 \pm 0.29$	$1.03 \pm 0.24$	$0.07 \pm 0.05$

and the last line gives the percentages of those orbits for which no resonance was found in the search with integer numbers up to 10. No resonant orbits with percentages larger than 1 per cent were found for integer numbers larger than 5. Notice that the resonances found here are the same found by Muzzio et al. (2009), except for the addition here of the (1, -2, 1) resonance which barely made it to Table 3 because its percentage is 1.07 in model E5.

As an example, Fig. 3 presents the  $x$ - $y$  and  $x$ - $z$  projections of orbit 1848 from model E4a, which corresponds to the resonance (3, -2, 0) type called fish.

#### 4 CONCLUSIONS

An interesting result from Paper I is that the different models in each group gave essentially the same results. The results of Table 1 show the same for the percentages of the different kinds of orbits: with very few exceptions (e.g. the percentages of OLATs in models E2b and E2c) the differences among models of the same group fall within the  $3\sigma$  level. Because of the small numbers involved, it is difficult to say if the same happens for the percentages of resonant orbits, because in order to obtain the results of Table 3 the three different models of each group had to be bunched together. Nevertheless, at least the plots in Fig. 1 do not show obvious discrepancies among the distributions of symbols that correspond to the different models.

The analysis of the present results should be done bearing in mind that all these models are dominated by chaotic orbits and that the regular orbits investigated here are just a minor component of the orbital content: about 22 per cent of all the orbits in models E2 and E5 and only about 13 per cent of the same in models E3 and E4. Thus, it is difficult to accept here the usual view that regular orbits provide the framework for these models and chaotic orbits just help to fill in the gaps, actually it seems to be the other way round.

The most abundant regular orbits turn out to be the SATs, in good agreement with the trend shown by a comparison of the results of Aquilano et al. (2007) and of Muzzio et al. (2009): the fractions of SATs increase several folds when going from non-cuspy to similar cuspy models. The percentages of SATs found here are even larger than those of the cuspy models of Muzzio et al. (2009), probably because the present models maintain the  $\gamma \simeq 1$  slope down to their innermost regions (see fig. 3 of Paper I), while the models of Muzzio et al. (2009) show some tendency to flatten near the centre of the systems. The increase of the fractions of SATs as one goes from the E2 towards the E5 models is in agreement with similar trends found

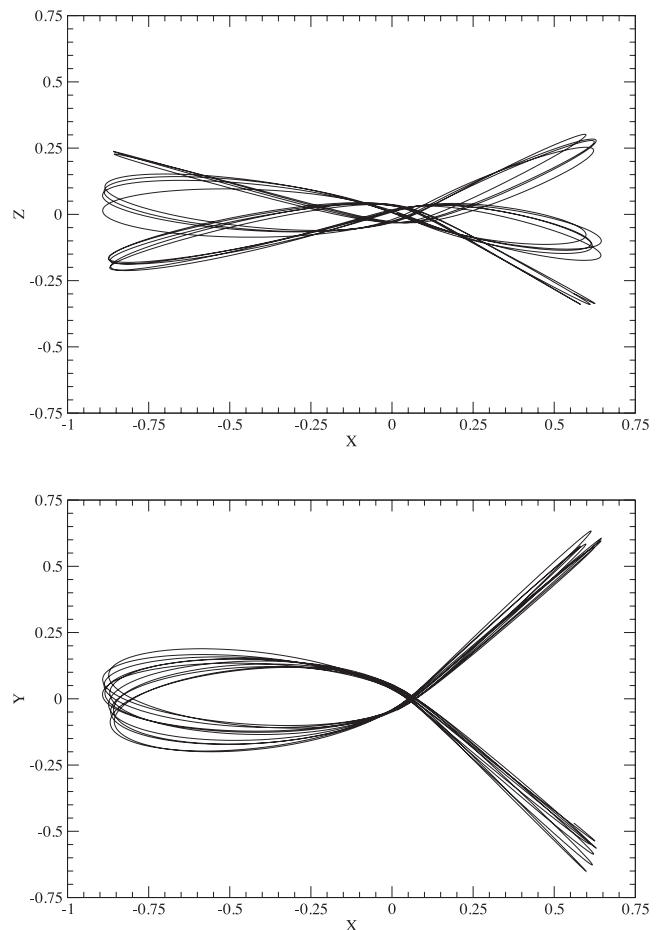


**Figure 3.** Projections on the  $x$ - $z$  (top) and  $x$ - $y$  (bottom) planes of resonant orbit 1848 from model E4a. The orbit obeys a (3, -2, 0) resonance, i.e. it is a fish.

by Aquilano et al. (2007) and Muzzio et al. (2009), respectively, for non-cuspy and cuspy models.

The large fractions of OLATs in the E2 models are probably due to the fact that those models have axial ratios  $b/a \simeq c/a$  in their outer regions, as shown in Table 2. For the other models, where the differences between the  $b/a$  and  $c/a$  ratios are larger, the fractions

of both ILATs and OLATs are very small, indeed. Similar trends were found by Aquilano et al. (2007) for non-cuspy models and by Muzzio et al. (2009) for cuspy ones.

The segregation of the orbits in energy bins shown in Table 2 reveals some interesting details, and one should bear in mind that orbital periods change enormously with energy, the orbits in the lowest energy bin having periods of the order of several tenths of t.u. and those in the highest of the order of several tens of t.u., i.e. a two orders of magnitude difference. The concentration of the newly detected chaotic orbits in the highest energy bin may thus be in part consequence of the use of a fixed time interval to compute the FT-LCNs in Paper I, and of a fixed number of periods to compute the orbital frequencies in the present paper. Nevertheless the fact that, in the sample of regular orbits from Paper I, those detected here as chaotic using a longer integration interval also show preference for the higher energy bins, shows that the effect is also in part real. In the case of sticky orbits, the effect is easy to understand because for the highest energy bins a fixed integration interval would involve less ‘periods’ of the chaotic orbit when it is behaving more or less regularly and, thus, less chance to detect its truly chaotic nature. For the weakly chaotic orbits, instead, there is no obvious selection effect and they are probably more abundant at high energies.

BBL orbits (recall that the bulk of them are not boxes, but boxlets) show a tendency to occupy the higher energy bins as we go from the E2 to the E5 models. Even though they represented less than one-third of the regular orbits in all the models (and in some of them much less than that), they are more than half of the regular orbits of the highest energy bin in models E4, and are almost as numerous as the SATs in the same bin of models E3. SATs, in turn, are less numerous in the highest energy bin but, except for the two mentioned cases, clearly dominate in all energy bins, as they do for all the energies taken together. As could be expected, OLATs tend to concentrate in the higher energy bins and they manage to outnumber the SATs in the highest energy bin of the E2 models. The opposite is true of the ILATs, but the tendency is less pronounced, and they are even fairly abundant in the highest energy bin of the models E2 where, as already indicated, those systems are close to being rotationally symmetric.

Most of the BBLs turn out to be resonant orbits. As could be expected from cuspy models, the fractions of boxes are very small and clearly diminish even further when the search for resonances is extended to larger integer numbers; it is worth recalling, however, that the bulk of the resonant orbits have resonances with integers not larger than 5. The  $(x, y)$  fishes, resonances  $(3, -2, 0)$ , are the most important boxlets in models E3 and E4, in agreement with the

results of Muzzio et al. (2009), but they are much less abundant in models E2 and E5 and, in fact, neither boxes nor boxlets seem to be of much relevance to models E2 and E5. Despite the differences between the fractions found here and those of Muzzio et al. (2009), it should be emphasized that the resonances whose fractions are larger than 1 per cent are essentially the same in both investigations: only resonance  $(1, -2, 1)$  was added here and it only exceeds 1 per cent in model E5.

## ACKNOWLEDGMENTS

We are very grateful to David Nesvorný for the use of his code and to R. E. Martínez and H. R. Viturro for their technical assistance. The suggestions of the referee, Luis Aguilar, were very useful to improve the original manuscript and are gratefully acknowledged. This work was supported with grants from the Consejo Nacional de Investigaciones Científicas y Técnicas de la República Argentina, the Agencia Nacional de Promoción Científica y Tecnológica, The Universidad Nacional de La Plata and the Universidad Nacional de Rosario.

## REFERENCES

- Aguilar L. A., Merritt D., 1990, *ApJ*, 354, 33  
 Aquilano R. O., Muzzio J. C., Navone H. D., Zorzi A. F., 2007, *Celest. Mech. Dyn. Astron.*, 99, 307  
 Binney J., 1982, *MNRAS*, 201, 1  
 Binney J., Spergel D., 1982, *ApJ*, 252, 308  
 Crane P. et al., 1993, *AJ*, 106, 1371  
 de Zeeuw T., 1985, *MNRAS*, 216, 273  
 Hernquist L., Ostriker J. P., 1992, *ApJ*, 386, 375  
 Kalapotharakos C., Voglis N., 2005, *Celest. Mech. Dyn. Astron.*, 92, 157  
 Kandrup H. E., Siopis C., 2003, *MNRAS*, 345, 727  
 Miralda-Escudé J., Schwarzschild M., 1989, *ApJ*, 339, 752  
 Moller P., Stiavelli M., Zeilinger W. W., 1995, *MNRAS*, 276, 979  
 Muzzio J. C., 2006, *Celest. Mech. Dyn. Astron.*, 96, 85  
 Muzzio J. C., Navone H. D., Zorzi A. F., 2009, *Celest. Mech. Dyn. Astron.*, 105, 379  
 Ryden B. S., 1996, *ApJ*, 461, 146  
 Sidlichovský M., Nesvorný D., 1997, *Celest. Mech. Dyn. Astron.*, 65, 137  
 Statler T. S., 1987, *ApJ*, 321, 113  
 Statler T. S., Emsellem E., Peletier R. F., Bacon R., 2004, *MNRAS*, 353, 1  
 Zorzi A. F., Muzzio J. C., 2012, *MNRAS*, 423, 1955 (Paper I)

This paper has been typeset from a  $\text{\TeX}/\text{\LaTeX}$  file prepared by the author.